AUTHOR(S): MUHAMMAD-SUKKI, F., ABU-BAKAR, S.H., RAMIREZ-INIGUEZ, R., MCMEEKIN, S.G., STEWART, B.G., MUNIR, A.B., YASIN, S.H.M. and RAHIM, R.A.

TITLE: Performance analysis of mirror symmetrical dielectric totally internally reflecting concentrator for building integrated photovoltaic systems.

YEAR: 2013

Publisher citation: MUHAMMAD-SUKKI, F., ABU-BAKAR, S.H., RAMIREZ-INIGUEZ, R., MCMEEKIN, S.G., STEWART, B.G., MUNIR, A.B., YASIN, S.H.M. and RAHIM, R.A. 2013. Performance analysis of mirror symmetrical dielectric totally internally reflecting concentrator for building integrated photovoltaic systems. Applied Energy [online], 111, pages 288-299. Available from: https://dx.doi.org/10.1016/j.apenergy.2013.05.006

OpenAIR citation: MUHAMMAD-SUKKI, F., ABU-BAKAR, S.H., RAMIREZ-INIGUEZ, R., MCMEEKIN, S.G., STEWART, B.G., MUNIR, A.B., YASIN, S.H.M. and RAHIM, R.A. 2013. Performance analysis of mirror symmetrical dielectric totally internally reflecting concentrator for building integrated photovoltaic systems. Applied Energy [online], 111, pages 288-299. Held on OpenAIR [online]. Available from: https://openair.rgu.ac.uk

Performance Analysis of a Mirror Symmetrical Dielectric Totally Internally Reflecting Concentrator for Building Integrated Photovoltaic Systems

Firdaus Muhammad-Sukki [a,b,*], Siti Hawa Abu-Bakar [a,c], Roberto Ramirez-Iniguez [a], Scott G McMeekin [a], Brian G Stewart [a], Abu Bakar Munir [d], Siti Hajar Mohd Yasin[e], Ruzairi Abdul Rahim [f]

[a] School of Engineering & Built Environment, Glasgow Caledonian University, 70 Cowcaddens Road, Glasgow, G4 0BA Scotland, United Kingdom

[b] Faculty of Engineering, Multimedia University, Persiaran Multimedia, 63100 Cyberjaya, Selangor, Malaysia

[c] Universiti Kuala Lumpur British Malaysian Institute, Batu 8, Jalan Sungai Pusu, 53100 Gombak, Selangor, Malaysia

[d] Faculty of Law, University of Malaya, 50603 Kuala Lumpur, Malaysia

[e] Faculty of Law, Universiti Teknologi MARA, 40450 Shah Alam, Malaysia

[f] Faculty of Electrical Engineering, Universiti Teknologi Malaysia, 81300 UTM Skudai, Johor, Malaysia

* Corresponding Author. Tel: +44(0)141 331 8938, Fax: +44(0)141 331 3690

E-mail: firdaus.muhammadsukki@gcu.ac.uk/firdaus.sukki@gmail.com

Abstract: This paper presents a mirror symmetrical dielectric totally internally reflecting concentrator (MSDTIRC). Here, its electrical and optical performances are investigated for building integrated photovoltaic applications. This concentrator is designed to tackle two issues: (i) providing sufficient gain in order to increase the electrical output of a solar photovoltaic (PV) system, and (ii) reducing the size of the PV cell needed, hence minimising the cost of the system. These experiments carried out had the objective of investigating the characteristics of the cell with the concentrator, the angular performance of the structure, and the effect of temperature on the cell. In each case, the current-voltage (I-V) characteristics and the power-voltage (P-V) characteristics are plotted and analysed. An outdoor experiment was also conducted to verify the results obtained from the indoor experiments. The PV cell-MSDTIRC structure is capable of providing a maximum power concentration of 4.2x when compared to a similar cell without the concentrator. The

deviation of the concentration factor from the geometrical concentration gain (4.9x), is mainly due to manufacturing errors, mismatch losses and thermal losses.

Keywords: solar photovoltaic; building integrated photovoltaic systems; solar concentrator; mirror symmetrical dielectric totally internally reflecting concentrator.

1. Introduction

Solar energy is one of the renewable energy sources that has greatest potential. It has been reported that, by 2011, solar photovoltaic (PV) had been introduced in more than 80 countries and was considered the fastest growing power generation technology [1]. In 2011 alone, a staggering 30 GW was installed globally making the global total reach 70 GW – an increase of 79% when compared with the installation carried out in 2010 [1]. The European Union (EU), at the time, dominated the solar PV market (see Figure 1), led by Germany and Italy, amounting to about 37.8 GW of the total installed PV [1]. The installed PV capacity is dominated by grid-connected installations, mainly due to the introduction of feed-in tariff schemes [2]. The off-grid sector on the other hand has experienced a declining share each year [1].

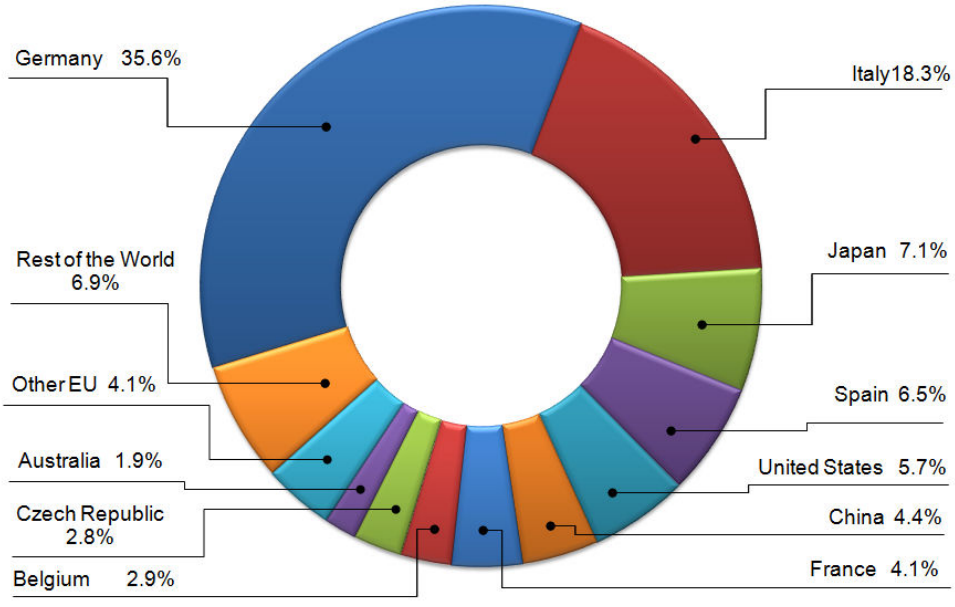

Figure 1: Top 10 Global PV market in 2011. Adapted from [1].

Recently, solar PV started to gain popularity in building integration applications [3]. It was estimated that between 20% and 40% of the world's energy consumption is consumed in commercial and residential buildings [4]. This figure is projected to experience an upward trend with an increase in the world population, a growth in building services and comfort levels as well as a rise in time spent in a building [4]. For this reason, governments worldwide are looking to design green buildings that can be energy efficient and independently generate energy [5]. Especially in urban environments, solar PV has potential not only for roof mounting, but also for integration in any building parts; i.e. the roof, facades and curtain walls, depending on the location and design of the building [6]. With an improved awareness on renewable energy, substantial financial incentives from governments and the downward trend of solar PV cost, the penetration of building integrated photovoltaic (BIPV) penetration is expected to rise sharply globally. China for example started the largest BIPV project in July 2010, with a capacity of 6.68 MW [7].

To further reduce the cost of the BIPV system, an application of PV devices is being introduced, known as the concentrating photovoltaic (CPV) system [8]. The CPV system utilises inexpensive optical devices to concentrate light from a large entrance aperture into a smaller exit aperture where a solar cell is attached [8]. Some of the benefits of the CPV systems include: a reduction in total cost of the system due to minimal usage of expensive PV material and a higher electrical output due to the increase in solar flux intensities at the solar cell [8]-[10].

Since 1970s, there are various CPV designs proposed by researchers worldwide. Sellami et al [9] proposed a CPV system called the Square Elliptical Hyperboloid (SEH) which has the potential to be integrated in double glazed windows. With a concentration value of 4x and acceptance angle of 120^{o} ($\pm 60^{o}$), an optical efficiency of 40% was recorded. Mammo et al. [11] investigated a reflective 3D crossed compound parabolic-based photovoltaic module (3D CCPC PV). This design is capable of generating a maximum power concentration of 3.0x when compared to similar type of non-concentrating module. Sarmah et al. [12] constructed a CPV system known as the Asymmetric Compound Parabolic Concentrator (ACPC) which generates a maximum power of 1.6 W, 2.1 times the power generated by the non-concentrating counterpart.

With a recent downwards trend of solar module price worldwide, the CPV system could still offer some added advantages; namely illumination, hot water and space heating generation, and ventilation. Illumination is achieved by implementing transparent/semi-transparent solar concentrators which allows the daylight to penetrate into the building hence reducing the energy requirement of the building [13]. Among the applications include sky lighting, windows and glass facades [3].

To ensure that the CPV system is working at an optimum level, it is cooled either by water

or air. Cooling using water is carried out by attaching a pipe at the bottom of the PV cell, where the heated water is collected and could be used as hot water and for space heating [14]. Cooling by air is achieved by combining the laminar flow effect and the chimney effect, creating good air ventilation for the building [14]. These processes allows the CPV system not only to generate electricity, but also the capability of producing hot water, space heating, ventilation and illumination, which further reduces the electricity requirement in a building, making it more desirable [14]-[17].

This paper proposes a new type of solar concentrator, known as a mirror symmetrical dielectric totally internally reflecting concentrator (MSDTIRC), for use in BIPV systems. Section 2 describes the fabrication process of an MSDTIRC, followed by the experimental setup, which is explained in Section 3. The experimental results are presented and discussed in Section 4. Finally, conclusions are presented in section 5.

2. Fabrication of MSDTIRC

The MSDTIRC is a new variation of DTIRC and is patent pending [19]. This concentrator is able to achieve different field of views on different planes. In contrast to the rotational axis symmetrical DTIRC proposed by Ning et al. [18], this new design generates a mirror symmetry design in four axes parallel to the base of the concentrator. The process used to fabricate an MSDTIRC is summarised in Figure 2.

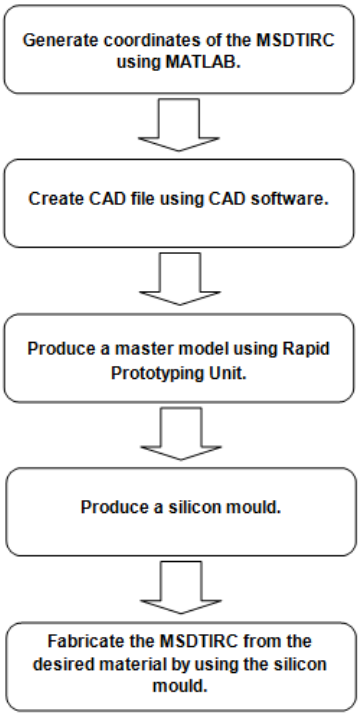

Figure 2: The process of fabricating the MSDTIRC.

A MATLAB® based program has been developed to create the MSDTIRC. The MSDTIRC uses the DTIRC based on the phase conserving method (PCM) [18] as the design's foundation and the process to produce this design is detailed out in Ref. [19]. Unlike the 3-D rotationally symmetry DTIRC that has a smooth dome shape entrance front surface, this design has a varying front surface with four axis of mirror symmetry (see Figure 3(d)). Depending on the input parameters, the front surface will be different from each design [19]. Another important characteristic of this concentrator is its square exit aperture, as presented in Figure 3(e). According to Sellami and Mallick [20], from the manufacturing point of view, it is desirable and easier to fabricate a square/rectangular cell, unlike a circular cell employed in a rotationally symmetry design.

From the MATLAB® code, the surface's Cartesian coordinates of the design are generated. These coordinates were imported into the GeoMagic® 3D software to produce a Computer-Aided Design (CAD) file as illustrated in Figure 3. From the CAD file, the design was transferred to a Polyjet™ technology's Rapid Prototyping Unit (RPU) known as the Objet Eden 350; a 3D printing system used to produce a master model. This technology is capable "to achieve ultra thin layers (0.016mm) enabling smooth, accurate and highly detailed models" to be constructed from a variety of materials [21].

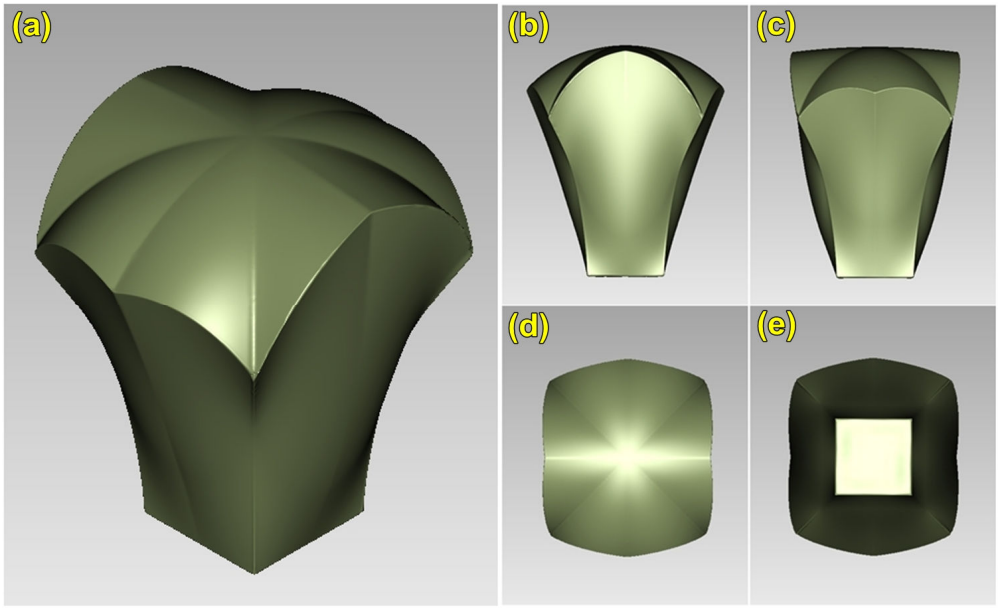

Figure 3: MSDTIRC (*HTot* = 3.0 cm, $\theta_{a\text{-}x} = 30^{o}$, $\theta_{a\text{-}z} = 40^{o}$, $n = 1.5$), where (a) is the isometric view; (b) is the side view 1; (c) is the side view 2; (d) the aerial view, and (e) is the bottom view of the concentrator.

The material used for the 3D printing is a liquid photopolymer resin [22]: an acrylic transparent material called Objet FullCure720™. This resin was chosen due to its good dimensional stability and surface smoothness. The photopolymer resin and gel-like support material are jetted on the tray layer by layer, with each layer of the photopolymer cured by ultraviolet (UV) light instantaneously after it is jetted, producing a fully cured model that can be handled and used immediately [22]. Once the master model is complete, the support material is easily removed by water jetting [22]. Figure 4(a) shows the master model generated from the RPU. This master model is then polished manually to an 'acceptable' degree to ensure the profile is smooth, as illustrated in Figure 4(b).

This master model is later used to produce a silicon mould. First, parting lines are set up on the master model using coloured tape. Once the feed and risers are constructed, the master model is then suspended in a mould casting frame. A silicon rubber mixture is prepared and is degassed in the bottom part of the vacuum casting machine. The silicon mixture is then poured into the mould casting frame and is put again in the bottom part of the vacuum casting machine for the second degassing process. The vacuum chamber ensures that all remaining air is removed from the silicon mould. Once the silicon is solidified (normally around 12 – 15 hours), the master model is removed from the silicon mould by cutting along the parting lines. The mould is later closed and sealed (either using tape or staples) and is ready to be used. The silicon mould is shown in Figure 4(c).

The next step is to produce the MSDTIRC from the desired material (also known as resin).

Material 6091 (manufactured by Renishaw PLC) was selected since it is rigid, water clear and transparent. It can also withstand high temperatures (up to 75^{o}C), is UV stable, has a refractive index of 1.515 and a transmissibility of 93.7%.

The vacuum casting process is described in detail in [23] and [24]. The 6091 resin is prepared in the top part of the vacuum chamber machine while the silicon mould is placed at the bottom part of the machine. The mixing process and pouring into the silicon mould are conducted via computer-controlled equipment. Again, the air is removed completely since the whole process takes place in vacuum. The final form of the MSDTIRC is produced from the solidified resin after the casting process is complete, as presented in Figure 4(d). The silicon mould could be used again in the future to produce subsequent copies either using similar or different resins.

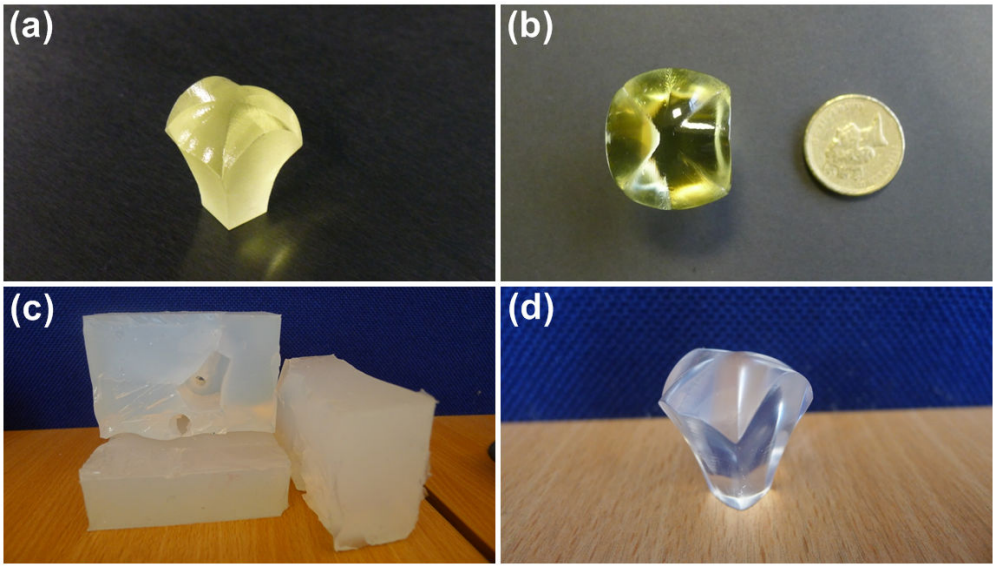

Figure 4: Outcome from the fabrication process, where: (a) the unpolished master model; (b) top view of a polished master model compared to a £1 coin; (c) a silicon mould, and (d) the final prototype of an MSDTIRC produced from 6091 material.

3. Indoor experiments.

There are three main pieces of equipment used in the experiments: (i) a Sun 2000 solar simulator (Class A AM1.5G irradiation spectrum) from Abet Technologies; (ii) a Keithley 2400 source meter, and (ii) a personal computer installed with National Instruments® software, as shown in Figure 5. The solar simulator provides a spectrum similar to the sun [25]. Unlike real outdoor conditions where the solar intensity and ambient conditions vary continuously, the indoor sun

simulator allows these factors to be controllable so their effects on the PV cell can be investigated. A Keithley 2400 source meter performs a similar operation to the loading circuit, but with more accuracy. All the data from the source meter is transferred to and stored in a personal computer installed with the National Instruments® software, which will plot the desired graph(s) for further analysis.

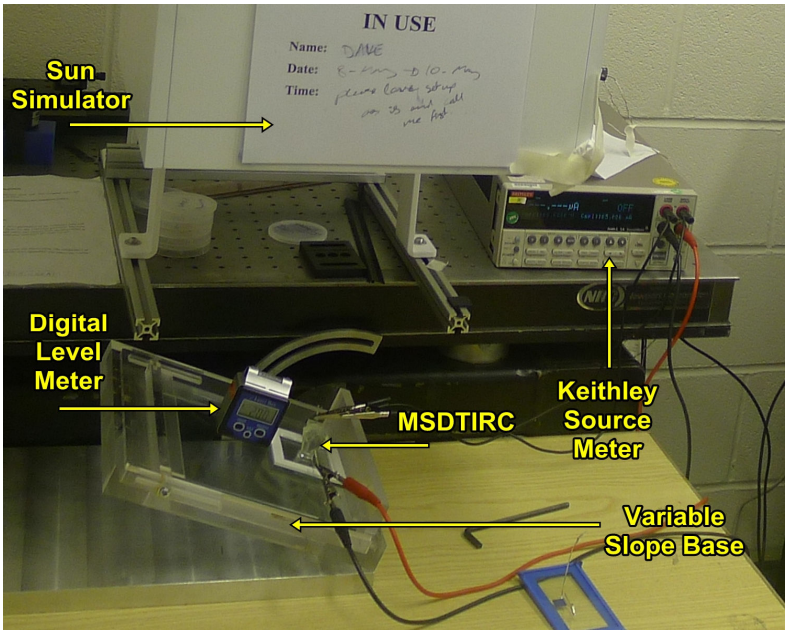

Figure 5: Indoor experimental setup.

The two square solar cells used in this experiment have an area of 1 cm^2 each. The solar cells are made from monocrystalline silicon (fabricated by conventional one-sun manufacturing processes) with an electrical conversion efficiency of 17.32%. Each solar cell is glued permanently on a separate glass that acts as the back substrate. The dimensions of the glass are (60 mm x 60 mm x 4 mm). The fabricated MSDTIRC is then mounted on one of the cells. Both samples (solar cells with and without the MSDTIRC) are used in all the experiments. Each sample is placed on top of a variable slope base which can be tilted between 0^o to 90^o. The tilt angle is determined by using the digital level meter.

3.1. Investigation of the Current–Voltage and Power–Voltage Characteristics of the MSDTIRC

The first experiment was carried out to investigate the current-voltage (I-V) and power-

voltage (P-V) characteristic of the MSDTIRC. The radiation intensity output of the solar simulator is set to be 1,000 W/m^2. The room temperature is set to 25^{o}C and the door of the room is closed to avoid unwanted air flow and minimise temperature variations. The variable slope base is set to be 0^o. In each experiment, a set of 200 reading of the voltage and current are taken, and the open circuit voltage (V_{oc}), short circuit current (I_{sc}), maximum voltage (V_{max}), maximum current (I_{max}), maximum output power (P_{max}) and fill factor (FF) are determined and calculated.

The first part of the analysis is to investigate the optoelectronic gain of introducing an MSDTIRC on the solar cell. A thin layer of Vaseline is applied between the MSDTIRC and the solar cell to create a temporary connection as well as removing any air gap between the cell and the concentrator, which would create unwanted reflections. The index of refraction of the Vaseline is 1.521 [26].

The I-V characteristic and the P-V characteristic of the MSDTIRC and a flat solar cell are presented in Figure 6. The opto-electronic gain is obtained by dividing the electrical signal, i.e. the short circuit current, generated from a solar cell with a concentrator (placed on top of the solar cell) by that of a solar cell without a concentrator [18]. The experiment shows that the MSDTIRC causes the short circuit current to increase by a factor of 4.2, from 37.4 mA to 157.7 mA. Similarly, the maximum power is also increased by more than four-folds, from 17.3 mW to 79.7 mW. The MSDTIRC manages to increase the fill factor slightly from 78.5% to 79.7%.

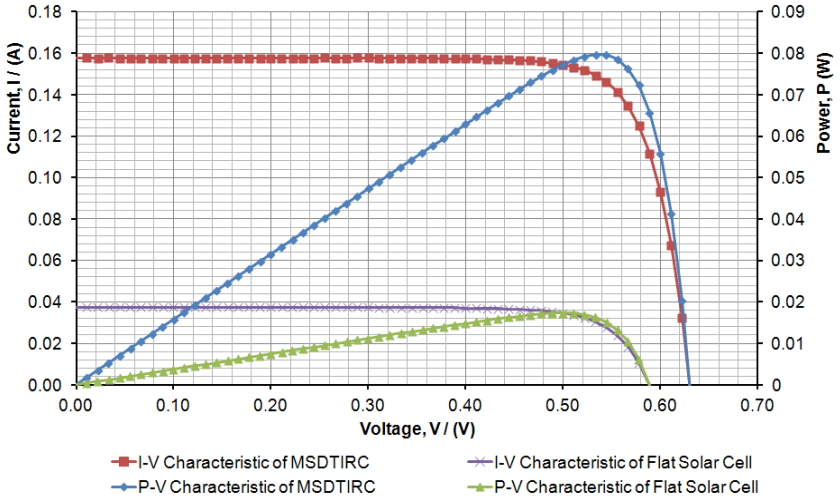

Figure 6: The I-V characteristic and the P-V characteristic of the MSDTIRC and a flat solar cell.

It is also useful to investigate the effect of not using an index matching gel. The experiment

is repeated by removing the Vaseline from the concentrator, and the experimental data is presented in Figure 7. It was found that the opto-electronic gain is reduced by about 12% when the Vaseline is removed from between the cell and the MSDTIRC. The short circuit current becomes 139.8 mA while the maximum power is reduced to 70.3 mW. This is mainly because the absence of gel introduces an air gap, causing some of the rays not to be fully transmitted to the PV cell. It is therefore recommended to apply a gel in between the concentrator and the PV cell.

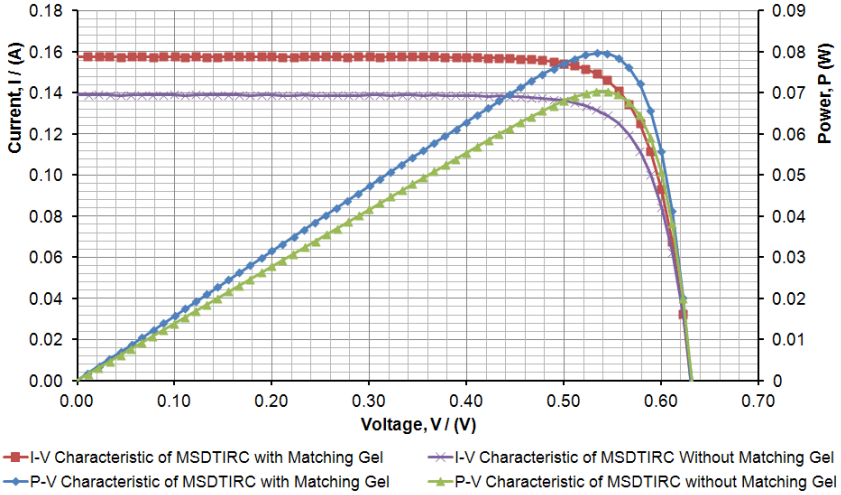

Figure 7: The I-V characteristic and the P-V characteristic of the MSDTIRC with and without index matching gel.

The next step is to investigate the performance of the MSDTIRC as well as the flat solar cell when each of them is illuminated under various levels of solar radiation. The experiment is repeated using solar radiation values ranging from 800 W/m^2 until 1,100 W/m^2. For each calibration of radiation, the solar simulator is left to achieve steady state for approximately 40 minutes. Figure 8 shows the I-V characteristic of the MSDTIRC and the flat solar cell while Figure 9 illustrates the P-V characteristic of both systems under various levels of solar radiation.

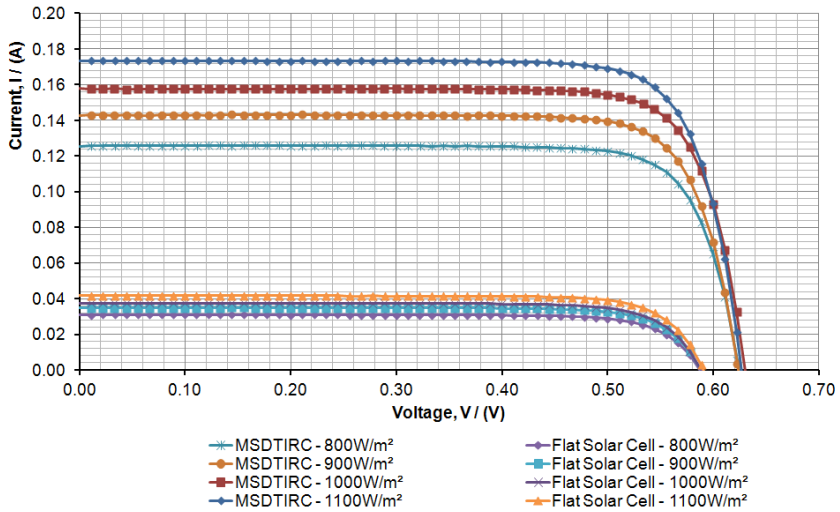

Figure 8: The I-V characteristic of an MSDTIRC (with index matching gel) and a flat solar cell under various levels of irradiance.

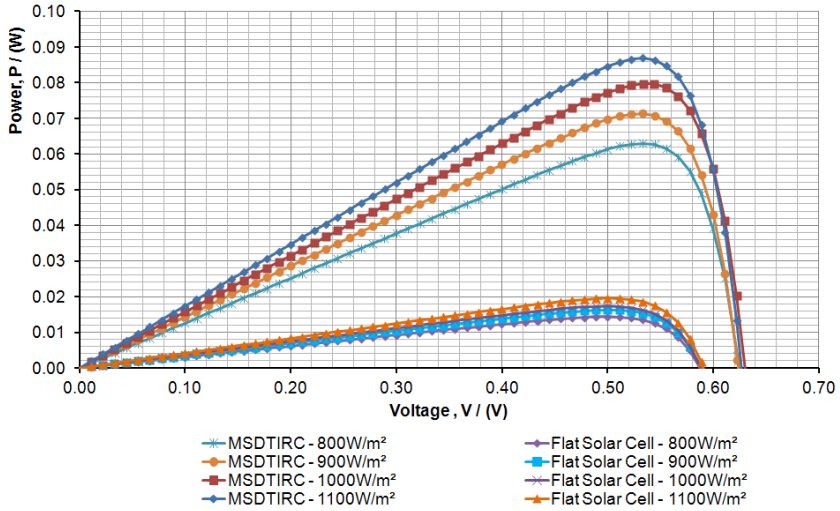

Figure 9: Variation of instantaneous power of an MSDTIRC (with index matching gel) and a flat solar cell under various solar irradiance values.

Looking at Figure 8, the short circuit current of the MSDTIRC increases by approximately 38% (from about 125.7 mA to 173.5 mA) when the intensity of the solar simulator is varied from 800 W/m^2 to 1100 W/m^2. Meanwhile, for the flat solar cell, the increment in terms of short circuit current is recorded from 30.9 mA to 41.6 mA. A similar trend is also observed for the output power of the cell, as illustrated in Figure 9. The maximum power of the MSDTIRC increases by 1.38 times (from 62.9 mW to 86.9 mW) when the solar radiation increases from 800 W/m^2 to 1,100 W/m^2. For the flat solar cell, this value improves from 14.4 mW to 19.5 mW.

In general, it is observed that the value of the short circuit current is directly proportional to the amount of solar radiation received by the cell. However, the intensity of the light has minimal effect to the open circuit voltage[1].

3.2. Angular Response of the MSDTIRC

Experiment to obtain the angular response of the structure, and investigate the effect that varying the angle of incidences of the incoming rays has on the electrical output of the cells, were also carried out. Before starting the experiment, it is desirable to fix the MSDTIRC permanently on a flat solar cell. A silicone elastomer Sylgard-184® from Dow Corning was chosen as the binding material to fix the concentrator to the top of the solar cell [12]. Besides having excellent transmission properties, another advantage of using this material is that it involves a simple curing process [12],[28]. To prepare the Sylgard, first, the supplied base and the curing agent is weighed in a 10:1 ratio and mixed in a small beaker. The mixture is then put in a vacuum chamber for approximately 10 minutes to eliminate air bubbles. Afterwards, the mixture is poured on top of the glass where the solar cell has been mounted. Once the solar cell and encapsulation material are in place, the MSDTIRC is placed carefully on top of the solar cell. The elastomer in the system is then cured in the oven for 1 hour at a temperature of 100^{o}C to ensure good binding between the MSDTIRC and the cell [28].

The experimental setup is shown previously in Figure 5. The sun simulator is set to exhibit an irradiance of 1,000 W/m^2, when the room temperature is at 25^{o}C. Instead of changing the rays' angle, the variable slope base is tilted accordingly. The tilt angle is measured accurately using a digital tilt meter. The measurements of the voltage and current are taken, for an angle of inclination starting from 0^{o} to 50^{o}, with intervals of 5^{o}. From each set of measurements, the open circuit voltage (V_{oc}), short circuit current (I_{sc}), maximum voltage (V_{max}), maximum current (I_{max}) and maximum output power (P_{max}) are determined and calculated. Then, the short circuit current and maximum output power are plotted against the inclination angle, and are presented in Figure 10 and Figure 11 respectively.

[1] From the experiments, the changes in open circuit voltage for the selected irradiance level are relatively small. However, note that the open circuit voltage is increasing logarithmically with respect to the intensity of the light [27].

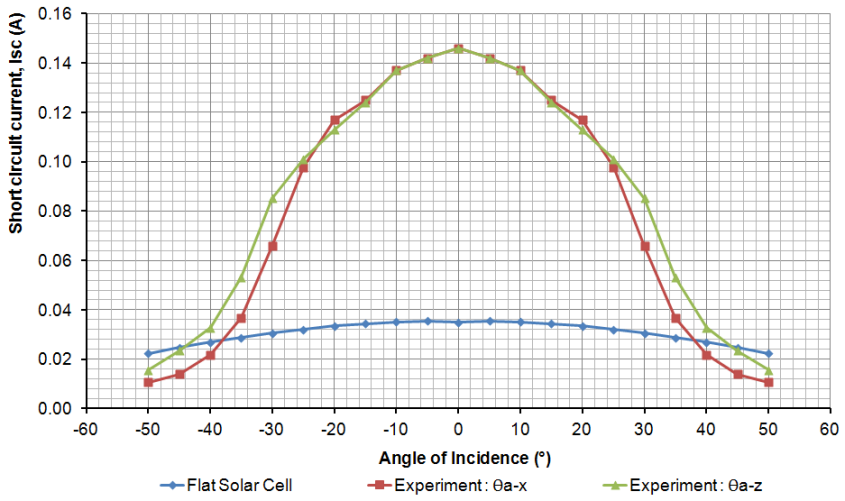

Figure 10: The short circuit current of MSDTIRC and flat solar cell at different angles of incidence.

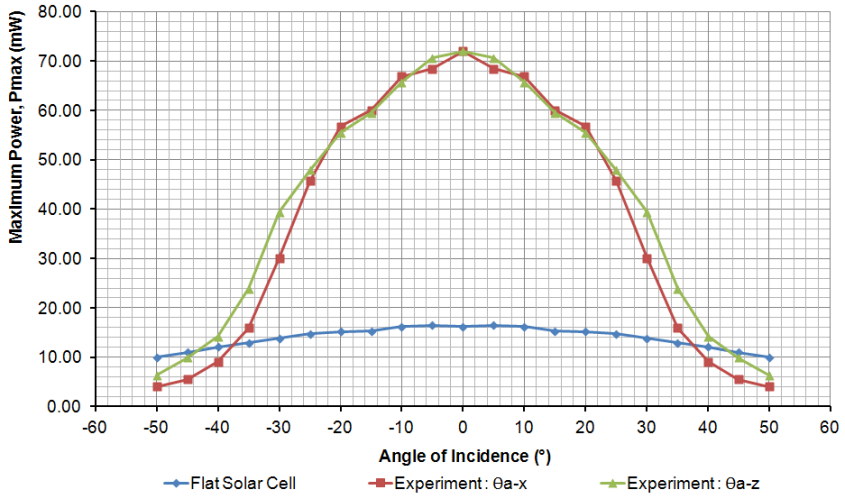

Figure 11: The maximum output power of MSDTIRC and flat solar cell at different angles of incidence.

From Figure 10 and 11, the maximum reading of both the short circuit current and the maximum power of the MSDTIRC are observed at 0^{o} inclination, with the reading of 146 mA for the short circuit current and 72 mW for the maximum output voltage. When the tilt angle is increased, both parameters show a gradual decrease. The output from the MSDTIRC reach 90% of its peak value (131.5 mA for the short circuit current and 64.8 mW for the maximum power) when the angle of incidence along the x and z-plane are 12^{o}. For the measurement along the x-axis, the readings of these two parameters drop to about 40% of their peak value (66 mA and 30 mW) when the inclination angle equal to the acceptance angle along the x-plane of 30^{o}. For the measurement along the z-axis, the readings of these two parameters drop to about 20% of their peak value (33 mA and 14 mW) when the inclination angle equals to the acceptance angle along the z-plane of 40^{o}.

To investigate the opto-electronic gain of the concentrator, the MSDTIRC's short circuit current is divided by the flat solar cell's short circuit current, and the results are plotted in Figure 12. From Figure 12, it can be observed that within the acceptance angles of the MSDTIRC, the opto-electronic gain is always more than 1.2 when compared with the flat solar cell, where the peak value calculated from the experiment is 4.17. The corresponding peak value from the simulation is the peak value from the optical concentration gain, i.e. 4.59, indicating a deviation of about 9%. The results from the experiment show good agreement with the simulation data. Some of the possible reasons for the deviation between the experiment and simulation values include manufacturing errors such as uneven surfaces of the entrance aperture and over polishing on the profile of the side wall, misalignment between the exit aperture of the concentrator and the solar cell, and reflection on the front surface of the MSDTIRC.

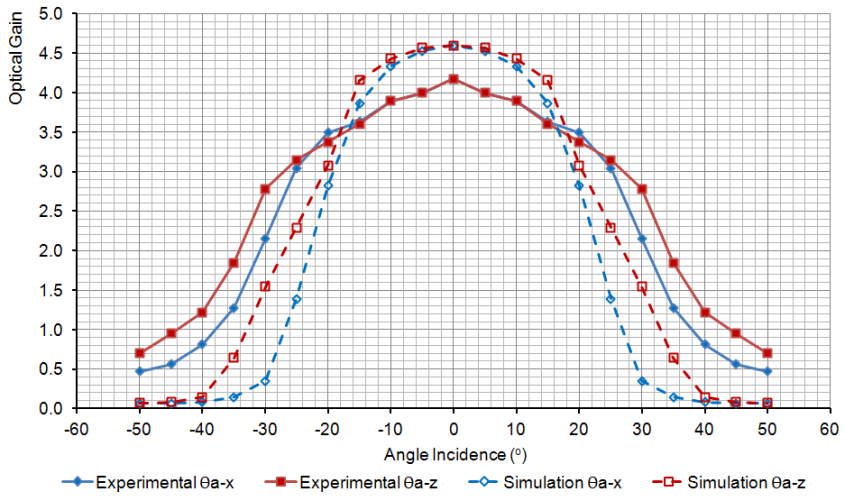

Figure 12: Optical gain of the MSDTIRC.

3.3 Thermal Characteristic of the MSDTIRC

To investigate the thermal characteristics of the MSDTIRC-PV structure, a thermocouple is placed under the bottom glass directly below the 1 cm^2 cell. A thermometer is also placed in the room to measure the room temperature. Before the start of the experiment, the door is closed to avoid any air flow which may transfer the heat from the external surface [25]. The sun simulator is set to produce a 1,000 W/m^2 irradiance level and the MSDTIRC is placed under constant illumination for 5 hours. The measurement was taken at intervals of 30 minutes.

Figure 13 illustrates the I-V characteristic of the MSDTIRC-PV structure with variation of temperature. In general, the temperature causes a significant change to the open circuit voltage of a

solar cell, but the change in the short circuit current is minimal [29].

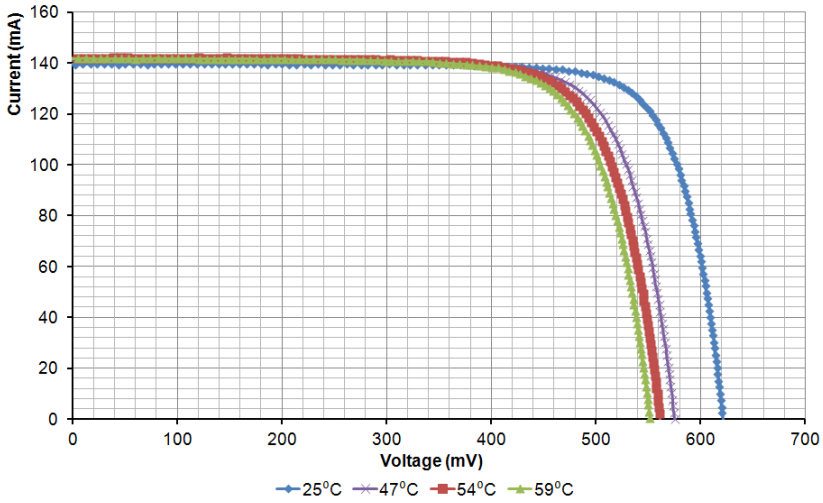

Figure 13: The I-V characteristic of the MSDTIRC at different cell temperatures.

A summary of the results is presented in Table 1. Throughout the duration of the experiment, the maximum value of the cell's temperature was recorded to be 58^{o}C, from the initial value of 25^{o}C. The value of maximum current remain the same throughout the duration of experiment, but the maximum voltage experiences a large drop from 526 mV to 456 mV after 5 hours of exposure. A similar decreasing trend is recorded in the maximum power and the fill factor value, a reduction from 69 mW to 60 mW and from 0.79 to 0.76 respectively. The decrease in power occurs abruptly and achieved a steady state value after 1.5 hours, as indicated in Figure 14. The temperature coefficient for maximum current, maximum voltage and maximum power can be calculated by taking the ratio of change in each parameter with respect to the change in temperature [11]. The calculated value of the maximum voltage coefficient is 2.1212 mV/^{o}C and the power coefficient is 0.2727 mW/^{o}C. Since no change is recorded in the maximum current, the current coefficient is 0.000 mA/^{o}C.

Table 1: Reading values for 5 hours of illumination for a solar intensity of 1,000 W/m^2.

Time (hour)	Temperature (^{o}C)	Maximum Power, P_{max} (mW)	Maximum Current, I_{max} (mA)	Maximum Voltage, V_{max} (mV)	Fill Factor FF
0.0	25	69	131	526	0.79
0.5	50	62	131	470	0.77
1.0	54	61	131	463	0.76
1.5	56	60	131	460	0.76
2.0	57	60	131	459	0.76
2.5	58	60	131	457	0.76
3.0	58	60	131	455	0.76
3.5	59	60	130	458	0.76
4.0	58	60	131	458	0.76
4.5	58	60	131	459	0.76
5.0	58	60	131	456	0.76

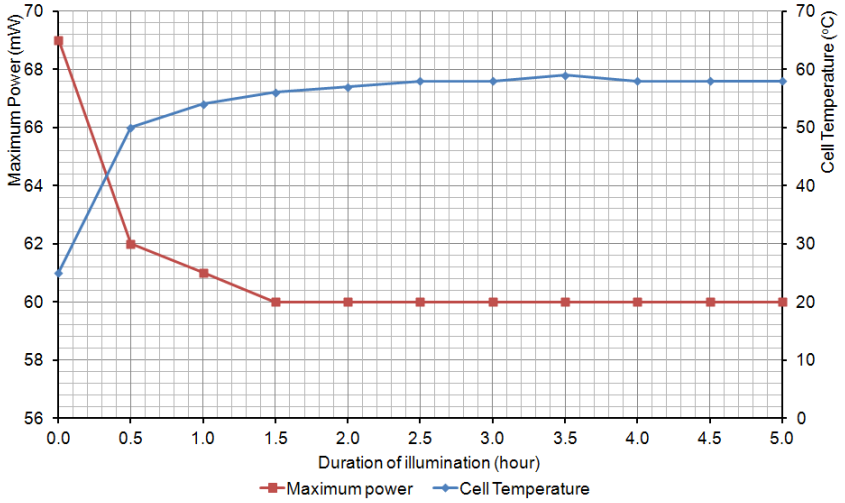

Figure 14: Variation of maximum power and the MSDTIRC cell temperature with illumination time.

4. Outdoor Experiments

The next step of the analysis involved conducting the experiment outdoor in an open environment. The chosen location for the outdoor test is located at a small park in St. Mungo Avenue, Glasgow (Latitude: 55.866^{o}N, Longitude: 4.247^{o}W). These experiments were conducted between 22 May 2012 and 28 May 2012.

The two samples (the MSDTIRC and a flat solar cell) are fixed on a hard surface board (21 cm x 30 cm). The board is then mounted on a tripod. A small elevation gauge is attached at the side of the board, and this gauge is used to measure the inclination of the board with respect to the vertical axis. To maximise the electrical output, the board is put in a south facing direction, with the

aid of a compass[2]. A multimeter is connected to each sample to get simultaneous readings. The multimeters measure the short circuit current produced by the cells at intervals of 5 minutes for a duration of 6.5 hours, i.e. from 9.45 am until 4.15 pm. Before the start of each experiment, the daily sun path and its elevation angle (with respect to the horizon) is determined from [30]. The experiments were conducted in four days:

- Experiment I: Sunny day at 0^o inclination with respect to the sun elevation angle.
- Experiment II: Cloudy day at 0^o inclination with respect to the sun elevation angle.
- Experiment III: Sunny day at 10^o inclination with respect to the sun elevation angle.
- Experiment IV: Sunny day at 20^o inclination with respect to the sun elevation angle.

For each experiment, a graph demonstrating the short circuit current of the MSDTIRC[3], the short circuit current of the flat solar cell and the opto-electronic gain is plotted.

In Experiment I, the board is tilted at 56^o to match the sun elevation angle to produce a 0^o inclination with respect to the sun elevation. It is observed that MSDTIRC produces a much higher short circuit current when compared with the flat solar cell for the whole duration of 6.5 hours, as illustrated in Figure 15. The peak gain of 3.86 is recorded at 1.00pm, with a value of short circuit current for the MSDTIRC and the flat solar cell of 141.1 mA and 36.5 mA respectively.

In Experiment II, the board is again tilted accordingly to ensure a 0^o inclination with respect to the sun elevation. The measured data from this experiment is presented in Figure 16. During the cloudy day, a large fluctuation of the short circuit currents was observed throughout the day. The graph of the opto-electronic gain shows a similar trend, with the maximum gain recorded for the day being 3.72.

[2] The compass points to magnetic south. For more accurate reading, the placement of the panel must be facing 'true south'. The magnetic deviation for the experimental site location is 3.72^oW.

[3] The measurement of short circuit current is taken along the z-plane of the MSDTIRC. Along this plane, the acceptance angle of the MSDTIRC is $\pm 40^o$.

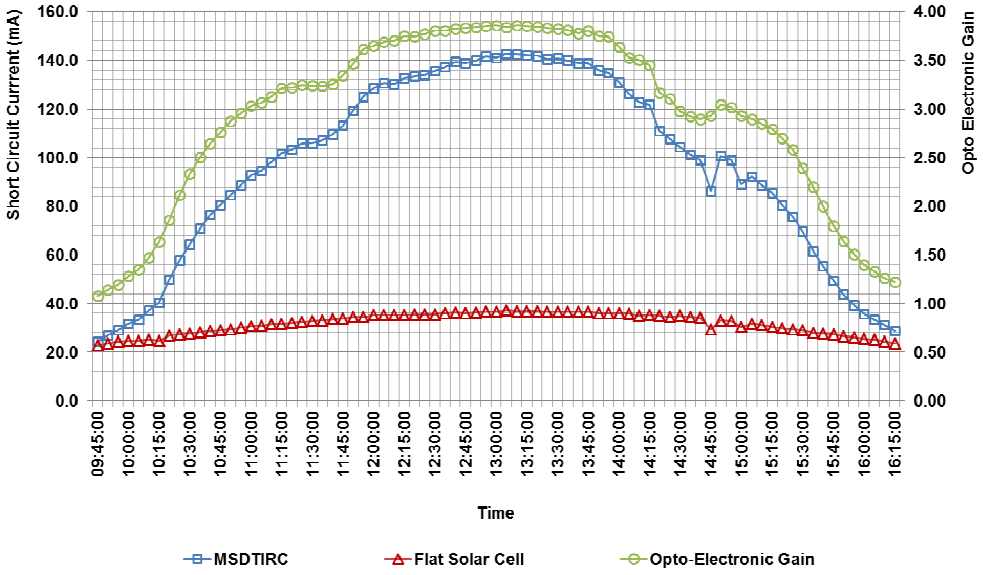

Figure 15: Comparison of short circuit current with and without concentrator as well as the optoelectronic gain for Experiment I.

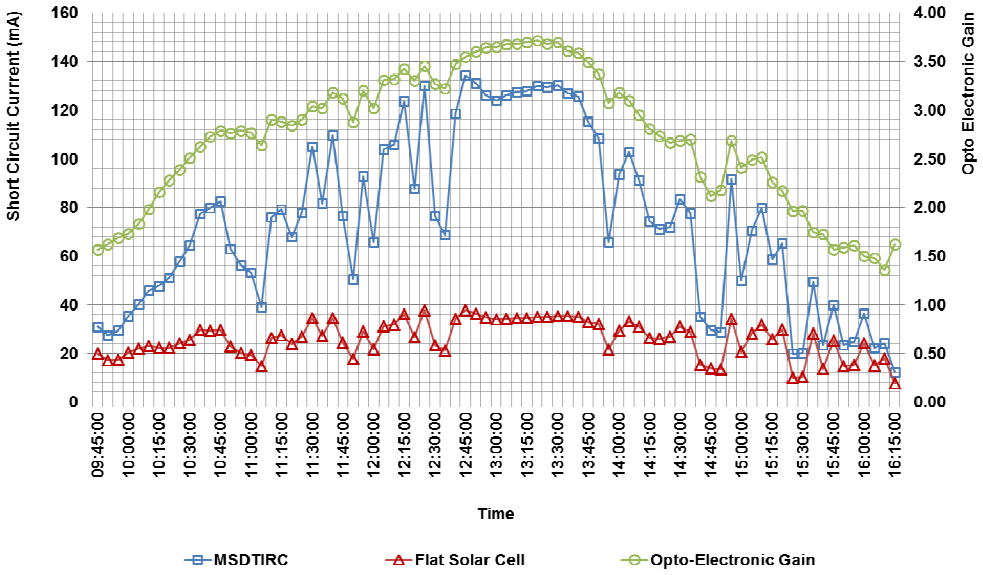

Figure 16: Comparison of short circuit current with and without concentrator as well as the optoelectronic gain for Experiment II.

It is understood that the altitude of the sun changes with the seasons. In four-season countries, the deviation of sun elevation varies greatly between summer and winter. Experiment III and Experiment IV are carried out to investigate the output of the MSDTIRC when the sun elevation changes. The tilt angle of the board is setup in such a way that the inclination angle is fixed at 5^{o} for Experiment III and 10^{o} for Experiment IV, with respect to the sun path. Figure 17

shows the results of Experiment III while Figure 18 shows the results of Experiment IV.

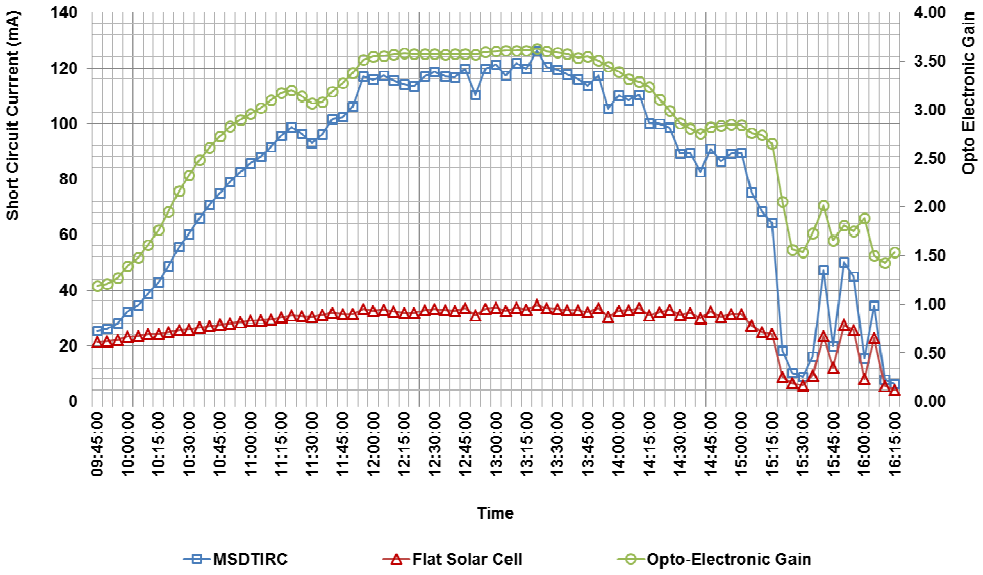

Figure 17: Comparison of short circuit current with and without concentrator as well as the optoelectronic gain for Experiment III.

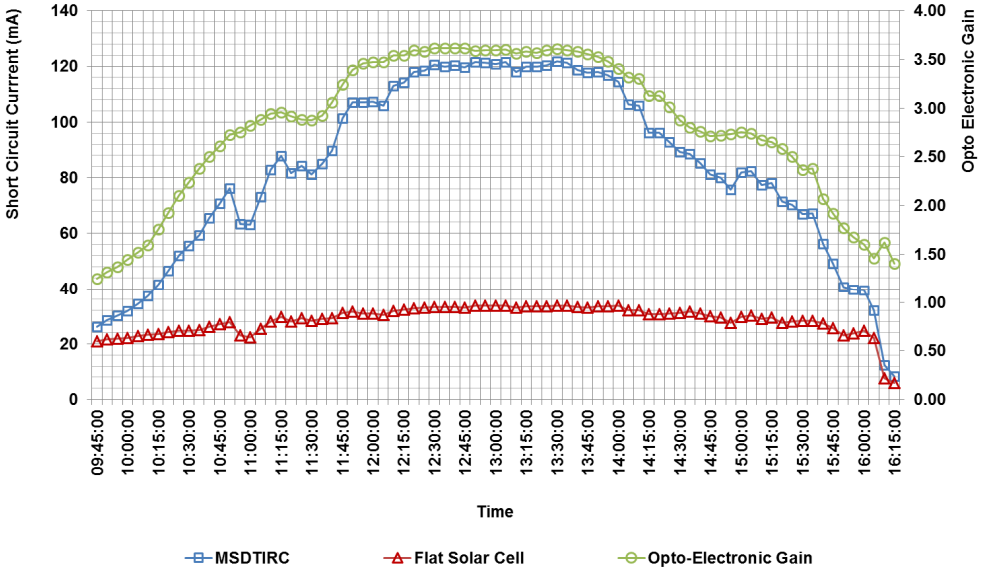

Figure 18: Comparison of short circuit current with and without concentrator as well as the optoelectronic gain for Experiment IV.

In Figure 17, the opto-electronic gain exhibits an almost identical trend to that exhibited in Experiment I until 3.15pm. Afterwards, the formation of clouds caused the short circuit currents to vary greatly. In Figure 18, the formation of clouds only occurred from 4.05pm onwards. As

expected, the maximum gain recorded for Experiment III and Experiment IV are lower when compared with Experiment I; with the maximum recorded values being 3.62 and 3.61 respectively.

It is observed that from all the experiments, the short circuit current generated by the MSDTIRC was always higher than the flat solar cell (for the 6.5 hour duration). This indicates that the MSDTIRC increases the electrical output from the cell during day time, with a gain of as high as 3.86. There is a mismatch between the highest gain for the indoor and outdoor test. Some of the reasons for this include misalignment of the concentrator with respect to the sun path, small errors in positioning the true south of the holding board, the constantly changing solar insolation, formation of clouds, as well as variation of wind speed which reduces the gain significantly.

5. Conclusions

One particular design of an MSDTIRC has been chosen to undergo a series of test. The fabrication process of this concentrator has been discussed thoroughly. Based on the prototype, a series of indoor experiments have been conducted to investigate the electrical performance of the MSDTIRC. The I-V and the P-V characteristics of the MSDTIRC have been evaluated and compared with a typical flat solar cell of a same dimension. An MSDTIRC manages to provide a maximum opto-electronic gain of 4.2x when compared with a flat solar cell. The angular response of the MSDTIRC was investigated and the results from the experiment show good agreement with the ZEMAX® simulation results. The thermal performance of the MSDTIRC has also been evaluated and it has been found that the maximum steady state temperature of the MSDTIRC for the experimental setup used was 58^{o}C. The calculated value of the maximum current coefficient, voltage coefficient, and power coefficient is 0.000 mA/^{o}C, 2.1212 mV/^{o}C and 0.2727 mW/^{o}C respectively. For the outdoor tests, the electrical performance of the MSDTIRC was observed for a period of 6.5 hours. A maximum opto-electronic gain of 3.86 was recorded during a sunny day with a 0^{o} inclination angle with respect to the sun elevation. It has been observed that the gain reduces when the tilt angle of the MSDTIRC with respect to the sun elevation angle increases. It can be concluded that the MSDTIRC has the capability to increase the electrical output of a solar panel when compared with a traditional solar cell. Within its acceptance angle, the gain of an MSDTIRC is much higher than that of a traditional solar cell. However, when the MSDTIRC concentrates the light on the cell, the temperature of the cell also increases. This affects the performance of the cell (attached to the MSDTIRC) where the power is reduced by about 13% when exposed under the sun simulator for a long period of time. Therefore it is necessary to cool the solar cell in order to obtain the maximum electrical output performance.

Acknowledgments

We would like to express our gratitude to Professor Tapas K Mallick and Mr Nabin Sarmah for their help in conducting the indoor experiments in Heriot-Watt University, Edinburgh, Scotland. Thanks are also due to Glasgow Caledonian University, the Scottish Funding Council and Yayasan TM for funding this research activity.

References

[1]. Renewable Energy Policy Network for the 21st Century (REN21), 2012. Renewables 2012 Global Status Report. REN21, Paris.

[2]. Ragwitz M, Held A, Stricker E, Krechting A, Resch G & Panzer C, 2010. Recent experiences with feed-in tariff systems in the EU – A research paper for the International Feed-in Cooperation. International Feed-In Cooperation, Europe.

[3]. Baig H & Mallick TK, Challenges and opportunities in concentrating photovoltaic research. Modern Energy Review 2011; 3(2): 20-26.

[4]. Prez-Lombard L, Ortiz J & Pout C. A review on buildings energy consumption information. Energy and Buildings 2008; 40(3): 394-398.

[5]. Mallick T, 2011. Solar energy research: Challenges and opportunities. MSc SES Seminar Day, Heriot-Watt University, Edinburgh.

[6]. Sick F & Erge T, 1996. Photovoltaics in buildings - A design handbook for architects and engineers. International Energy Agency Solar Heating and Cooling Programme, Earthscan.

[7]. RenewableEnergyFocus, 2010. BIPV on the upswing, RenewableEnergyFocus. Last accessed on [11/12/2012]. Available from http://www.renewableenergyfocus.com/view/11426/bipv-on-the-upswing/

[8]. Makrides G, Zinsser B, Norton M, Georghiou GE, Schubert M & Werner JH. Potential of photovoltaic systems in countries with high solar irradiation. Renewable and Sustainable Energy Reviews 2010; 14(2): 754-762.

[9]. Sellami N, Mallick TK & McNeil DA. Optical characterization of 3-D static solar concentrator. Energy Conversion and Management 2012; 64: 579-586.

[10]. Norton B, Eames PC, Mallick TK, Huang MJ, McCormack SJ & Mondol JD. Enhancing the performances of building integrated photovoltaics. Solar Energy 2011; 85(8): 1629-1664.

[11]. Mammo ED, Sellami N & Mallick TK. Performance analysis of a reflective 3D crossed compound parabolic concentrating photovoltaic system for building façade integration. Progress in Photovoltaic: Research and Applications 2012; http://dx.doi.org/10.1002/pip.2211.

[12]. Sarmah N, Ghosh A & Mallick TK. Indoor performance analysis of a low concentrating photovoltaic module for building integration. Proceedings of 8th International Conference on Concentrating PV Systems (CPV-8), Spain 2012; 110-113.

[13]. Sellami N & Mallick TK. Design of nonimaging static solar concentrator for window integrated Photovoltaic. Proceedings of 8th International Conference on Concentrating Photovoltaic Systems (CPV-8), Spain 2012; 106-109.

[14]. Clive B. Photovoltaic cell apparatus. Patent Number WO/2010/026415, 2009.

[15]. Muhammad-Sukki F, Ramirez-Iniguez R, McMeekin SG, Stewart BG & Clive B. Solar concentrators in Malaysia: Towards the development of low cost solar photovoltaic systems. Jurnal Teknologi 2011; 55(1): 53-65.

[16]. Muhammad-Sukki F, Ramirez-Iniguez R, McMeekin SG, Stewart BG & Clive B. Optimised dielectric totally internally reflecting concentrator for the Solar Photonic Optoelectronic Transformer System: Maximum concentration method. Proceedings of 14th International Conference on Knowledge-Based and Intelligent Information & Engineering Systems (KES 2010), Cardiff 2010. Part IV, LNAI 6279:633-641.

[17]. Kumar R & Rosen MA. A critical review of photovoltaic-thermal solar collectors for air heating. Applied Energy 2011; 88: 3603-3614.

[18]. Ning X, Winston R & O'Gallagher J. Dielectric Totally Internally Reflecting Concentrators. Applied Optics 1987; 26(2): 300–305.

[19]. Muhammad-Sukki F, Ramirez-Iniguez R, McMeekin SG & Stewart BG. Optical element. UK Patent Application No. GB1122136.3, 2011.

[20]. Sellami N & Mallick TK. Optical efficiency study of PV crossed compound parabolic concentrator. Applied Energy 2013; 868-876.

[21]. Department of Design Manufacture and Engineering Management (DMEM), 2012. Rapid Prototyping Facility. DMEM, University of Stratchlyde, United Kingdom. Last access on [16/12/2012]. Available from http://www.strath.ac.uk/dmem/businessandindustry/rapidprototypingandmanufacturingfacilities/rapidprototypingfacility/.

[22]. Objet, 2012. Last access on [16/12/2012]. Available from http://www.objet.com/3D-Printing-Materials/Overview/Transparent/.

[23]. Youtube, 2012. Vacuum Casting Video. Last access on [16/12/2012]. Available from http://www.youtube.com/watch?v=RnsepAK-V2o&feature=related

[24]. Manufacturing Engineering Centre, 2012. Last access on [16/12/2012]. Available from http://www.mec.cf.ac.uk/services/?view=vacuum_casting&style=plain

[25]. Mallick T, 2003. Optics and heat transfer for asymmetric compound parabolic photovoltaic concentrators for building integrated photovoltaics. PhD Thesis, University of Ulster, UK.

[26]. Synowicki RA. Suppression of backside reflections from transparent substrates. Physica Status Solidi (c) 2008; 5(5): 1610-1642.

[27]. Cai X, Zeng S, Li X, Zhang J, Lin S, Lin A & Baoping Z. Effect of light intensity and temperature on the performance of GaN-based p-i-n solar cells. Proceeding of International Conference on Electrical and Control Engineering (ICECE), 2011: 1535-1537.

[28]. Dow Corning, 2012. Sylgard® 184 Silicone Elastomer Kit. Dow Corning, USA. Last access on [16/07/2012]. Available from http://www.dowcorning.com/applications/search/products/details.aspx?prod=01064291

[29]. Yates TA, 2003. Solar cells in concentrating systems and their high temperature limitations. BSc Thesis, University of California, Santa Cruz.

[30]. University of Oregon - Solar Radiation Monitoring Laboratory, 2012. Sun path chart program. University of Oregon, USA. Last access on [16/12/2012]. Available from http://solardat.uoregon.edu/SunChartProgram.html.